

Geo-electric Investigation of the Cause of Structural Failure Indices on a Set of Administrative Blocks

Muslim B. Aminu

(Department of Earth Sciences, Adekunle Ajasin University Akungba-Akoko, Nigeria)

Abstract: *Electrical resistivity imaging has been employed to investigate the causes of structural failure related cracks on a set of administrative buildings in southwestern Nigeria. The goals were to determine the distribution of subsurface geologic lithologies beneath the set of buildings and therefrom infer the relative strengths of such lithologies. Data were collected along four geo-electric traverses using the ABEM1000 Terrameter unit. The dipole-dipole array was utilized with an electrode separation of 5 m. Observed field data were processed and inverted using a 2.5D finite-element modeling inversion algorithm. Results indicate that the northeastern half of the site is underlain by unweathered basement rocks overlain by thin (generally < 4 m) soil cover, while the southwestern region is dominated at depths beyond 4 m by low-resistivity water-saturated clays and some weathering tills. The clays apparently receive abundant supply of water from a seasonal stream channel adjacent to the westerly administrative blocks. The block presenting with the most damage has been built out over the edge of the shallow basement rocks onto these less competent water-saturated clays in the southeastern region resulting in cantilever-style differential settling. A second damaged block is situated entirely on low resistivity water-saturated clays. Differential settling on this block is likely related to the difference in thicknesses of the clays between sites of the north and south facing walls of the structure. Beneath the northern wall, the clays are thinner and could be expected to compress less than at the southern wall. Though uncalibrated to core or log data, the results allowed a first insight into possible causes of structural failure on the buildings and it is hoped that palliative measures will benefit from these results.*

Keywords: *basement scarp, electrical resistivity imaging, engineering site investigation, structural failure, water saturated clays.*

I. Introduction

Post construction structural failure indices which appear on engineering structures are adducible to two principal factors: 1) technical defects, which include deficient structural design and the use of inadequate quality materials and 2) inadequate information on the subsurface conditions of the construction site [1]. In well regulated societies, where building codes are well established and industry oversight is thoroughly implemented by relevant agencies, the latter rather than the former becomes the main culprit. The usual practice in the construction industry in investigating the subsurface conditions of the construction site is to resort to invasive near surface testing methods. These include soil testing and penetrative cone and tri-axial tests. However, these methods generally suffer a number of limitations; 1) general practice is to limit testing to the very near surface region (usually 1 – 4 m) and thus do not often provide information on the deeper subsurface (5 – 20 m) which could impact construction works negatively; 2) due to the prohibitive cost of testing, sample points are few and far in-between. They therefore do not present continuous lateral and vertical information on conditions of the subsurface and have the potential to totally miss out important geologic features in the subsurface particularly when sampling frequency exceeds the geometric dimensions of target features. In order to overcome these deficiencies, non-invasive geophysical techniques have often been used to compliment geo-technical testing procedures [2, 3]. The geo-technical tests provide hard-core incontrovertible data (albeit spatially sparse) while the geophysical techniques provide soft (requiring calibration) data with the required spatial coverage and density. It is even practicable to begin construction site investigation with the non-invasive geophysical techniques prior to the deployment of geo-technical testing [1]. Geophysical techniques are rather cheap and fast. They also provide a dense (in terms of detail) and geometric view of subsurface conditions allowing a thorough appreciation of the possible variations in bearing capacity of soils and the geologic features which could impact engineering structures.

One of the most versatile and oft-utilized geophysical methods in construction site investigation till date is Electrical resistivity imaging [4]. The method is relatively easy to implement; fast to acquire and interpret, and cheap. Responding to electrical contrast in the subsurface (which is mostly a result of the nature and amount of water in interstitial pore spaces in rocks and soils), the electrical resistivity method is capable of imaging a variety of geologic structures and features in the subsurface. Within basement terrains where soil cover is little developed, features such as fractures [5, 6, 7, 8, 9], deep weathering troughs [10], water saturated

clay bodies [11], underground caves [12, 13, 14] and buried objects such as tanks, pipes, cables are easily delineated [15, 16].

This study presents a geo-electric investigation of the subsurface lithologic distribution at the site of a set of administrative office complex on Adekunle Ajasin University Campus, Akungba-Akoko, which had begun to show signs of structural failure shortly after its construction and commissioning for use.

II. Site Of Investigation

The study site is located in the central campus of the Adekunle Ajasin University, Akungba-Akoko. Akungba-Akoko lies between Longitudes $05^{\circ} 43'$ and $05^{\circ} 47'$, and Latitudes $07^{\circ} 27'$ and $07^{\circ} 31'$ in the northeastern extremes of Ondo state in Nigeria (Fig. 1a).

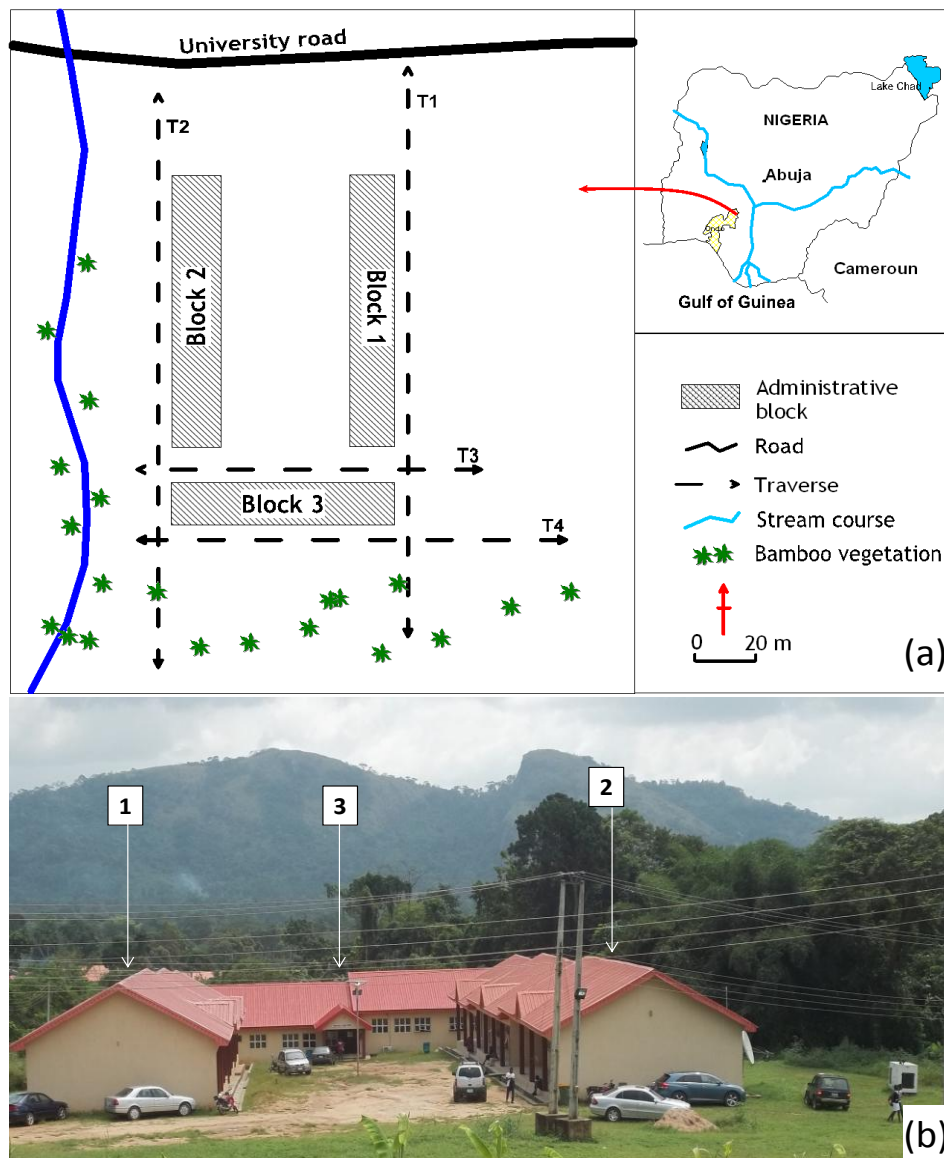


Fig. 1: (a) Location map of the survey area; and (b) North view of the U- complex

The area is underlain by rocks of the migmatite-gneiss suite of the basement rocks of southwestern Nigeria [17]. The rock suites of the area include biotite-rich gneisses, granite gneiss and charnokites. The rocks have experienced multiple tectonic episodes and developed an array of indicative relics such as faults, joints and extensive pygmatitic and minor drag folds. Topographic relief is averagely greater than 345 m above sea-level for most of the central portions of Akungba but perimeter hills rise up to 420 m above sea-level. Drainage is provided by a few mainly seasonal streams which take their source from high reliefs in the northeast. The courses of streams are controlled by major fracture systems which are sometimes expose to the surface.

The survey was taken around a U-complex of three administrative blocks (Fig. 1b) which house the Examination and Records unit, the Senate administrative annex and a string of science workshops. At the time of the survey, the west block hosted the Examination and Records unit, the east block a set of science workshops while the south block hosted the Senate administrative annex. The U- complex opens northwards towards a major university road. A few meters west of the complex lies a seasonal N-S trending stream whose course is dotted with the development of thick bamboo vegetation. The area is generally flat-lying with a very gentle southward slope. On the surface, soils are sandy and apparently well drained and do not indicate any presence of mixed rock aggregates.

III. Reason for this Study

During a routine administrative visit to the U- complex in 2013, hair-line cracks were observed on the interior walls of the southern block (Fig. 2a and b) of southerly block of the complex. These cracks were observed to span from the side of the doorway to the ceiling and occurred on virtually all rooms north of the central corridor of the building. Further observations revealed similar cracks on window frames of the north-facing wall of the building, some of which had been repaired (Fig. 2c). More extensive cracks were observed on the southern end of the eastern block (Block 1), a section which houses conveniences attached to the building. The cracks were restricted to the southern end on this block and included long vertical and lateral hair-line cracks on doorway, floors and internal and external walls (Fig. 2d - f). In the interior of the conveniences section, failure signs further included a sunken floor (Fig. 2g). No cracks were observed on the western block (Block 2). Since the building was only recently constructed and commissioned for use in 2012 and the University management known to be keen on construction standards, initial suspicion was that the observed signs of failure were most probably related to differential settling of the building as a result of variation in the load bearing strengths of subsurface materials at the site. Therefore it was decided that a geo-electric survey of the site be undertaken to obtain insight into possible variations in subsurface material and plausible causes of the observed failure indices.

IV. Methodology

A total of four (4) traverses were established in the study area. Traverse 1 (Tr. 1) was laid from south to north to the east of the most easterly block roughly 1.2 m from the building wall. Traverse 2 (Tr. 2) runs west of the westerly block from south to north. Both traverses were 120 m in length. Traverses 3 and 4 (Tr. 3 & 4) straddle the front and rear sides respectively of the southerly block and both run from east to west. Tr. 3 had a total length of 75 m while Tr. 4 was 95 m long. The spatial relationships of the four traverses are expressed in Fig. 1. Block 3 (the southerly block) was initially the main focus as failure cracks were first observed thereupon. Electrical resistivity data were collected using the ABEM 1000 Terrameter system. The dipole-dipole technique was utilized to capture both lateral and vertical variations in conditions of the subsurface. Dipole spacing on all traverses was 5 m and a maximum dipole length of 35 m was maintained throughout the survey. Data were collected in February, 2014, at the height of the dry season.

Field resistivity data were evaluated for spikes and data inversion was carried out using a 2.5D finite element modeling inversion algorithm (DIPROfWIN 4.01). The program utilizes the Active Constraint Balancing scheme to determine the spatially varying Lagrangian multipliers for the least-squares inversion algorithm [18]. It thus optimizes between robustness of the inversion result and smoothness of the inversion. The program inverts the data by minimizing the difference between an initial synthetic model of subsurface resistivity distribution and the observed resistivity fields until a reasonable fit is achieved. The inversion is deemed suitable and the iteration is stopped once the mismatch error drops below 5%. The program output three images, the observed field data pseudo-section, the computed theoretical data pseudo-section and the inverted subsurface resistivity structure. Considering the wide range of inverted resistivity (3.75 – 3755 Ohm-m) a logarithmic color display was utilized and display was limited to the range 49 – 1000 Ohm-m as these provided the best visual presentation of resistivity distributions along the traverses.

The 2D subsurface resistivity images along the traverses were interpreted for subsurface geology following criteria similar to the criteria of Aminu *et al.*, [8] and Aminu [11]. High laterally and or vertically continuous resistivities (usually above 350 Ohm-m) were interpreted to indicate unfractured basement rock. Low continuous-in-the-subsurface resistivities (usually below 82 Ohm-m) were interpreted to represent water



Fig. 2: Structural damage cracks on the U- complex buildings: (a) – (c) cracks on the interior and exterior walls of Block 3; (c) & (d) cracks on exterior walls of the conveniences of Block 1; and (f) & (g) lateral cracks and sunken floor in the interior of the conveniences of Block 1. Repaired cracks (red arrows); unrepaired cracks (black arrows) and sunken floor (yellow arrow)

Saturated deep-weathering clay-rich lithologies infilling trenches or fracture pathways. Moderate resistivities (usually 100 – 250 Ohm-m) were interpreted to represent one of two lithologies; 1) in the near surface they were regarded as well drained sands which can be visually observed at the survey site and 2) at depth they were regarded as weathering remains of the original bedrock poor in clays.

V. Results

Fig. 3 presents a composite display which consists of three images; the observed field data pseudo-section, the computed theoretical data pseudo-section and the inverted 2D resistivity structure beneath Traverse 1 (Tr. 1) location. This traverse is 1.2 m east of the walls of the east block (Block 1) of the complex. The robustness of the inversion can be gauged by the level of similarity between the resistivity distribution patterns in the observed field data pseudo-section and the theoretical data pseudo-section.

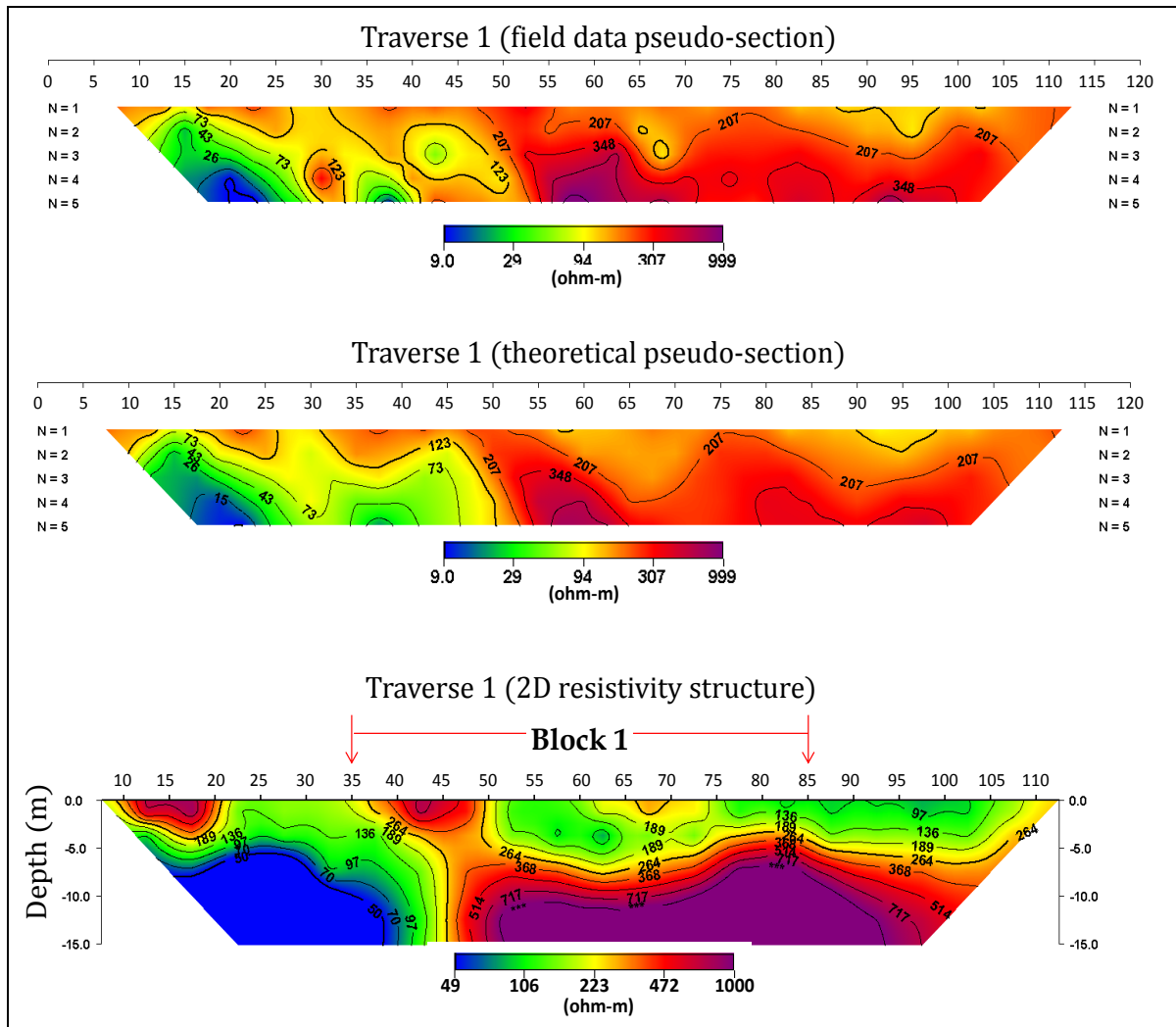


Fig. 3: Composite pseudo-sections of the results of 2D resistivity inversion along Traverse 1; (a) Observed resistivity data (b) Computed resistivity distribution; and (c) Inverted resistivity structure. At depth Block 1 has been built over the southern edge of the high resistivity basement rock response onto low resistivity clays. The location of Block 1 is indicated in red arrows.

The subsurface resistivity distribution beneath the Tr. 1 indicates continuous low to moderate resistivity responses in the near-surface all-through the length of the profile. This resistivity pattern generally ranges from 100 – 250 Ohm-m. This pattern is punctuated along the profile at positions 9 – 22 m, 35 – 50 m, and 62 – 73 m by even higher resistivity responses sometimes in excess of 350 Ohm-m. This low to moderate resistivity response has an average thickness of 5 m. At portions which appear as troughs this response reaches depths in excess of 5 m. In the southern extreme of the profile, the response may reach depths of up to 8 m. This pattern is interpreted to represent the *insitu*-weathering topsoil at the survey site. This topsoil is capped by loose sands at the survey site. Higher resistivity sections within this pattern possibly indicate sections of the topsoil richer in clayey fractions which have dried-out due to the long dry season. Some of these clay-rich soils can be observed at locations on the surface within the site. At deeper levels for most of the profile, specifically from position 45 m till the northern limit of the profile, the resistivity response is dominated by very high resistivities. This response extends from an average depth of 5 m downwards and has consistently high resistivity values generally in excess of 300 Ohm-m. The upper limit of this response consists of two trough-like depressions each roughly 1.5 m deep. The southern limit of this response is vertical at about the 45 m mark. This response was interpreted as the un-weathered bedrock at the site. Further southwards at depth, there exists a dome-shaped very low resistivity response with resistivities generally lower than 80 Ohm-m. Vertically, this response extends from an average depth of 5 m downwards and laterally, it extends from the southern limit of the profile till a little beyond the 40 m mark. The contact between this very low resistivity response and the adjacent higher resistivity response is vertical and sharp. This response pattern was interpreted as one of two possibilities: (1) deep-weathering water saturated *in-situ* clays which have developed in trench-like depressions in the bedrock of

the area (Aminu, 2015); or (2) clay-filled subterranean fluid migrations paths created by fracturing of the bedrock. To the latter effect, it is instructive that the contact between this response pattern and the adjacent high resistivity response interpreted as un-weathered basement is vertical. Also, the rocks of the area have experienced at least two deformational episodes which have resulted in the creation of numerous fractures and minor folds [17].

Fig. 4 is the inverted 2D resistivity structure beneath Traverse 2 (Tr. 2) location. This traverse is 1.2 m west of the walls of the west block (Block 2) of the complex and roughly 15 m east of the course of the seasonal stream in the area. The resistivity distribution beneath this profile is dominated by low to moderate resistivity responses in the range 80 -200 Ohm-m. It runs all-through the profile at shallow levels within the exception of locations 25 – 30 m and 98 m on to the northern limit of the profile. At these locations it is punctuated by very low resistivity near-surface materials with resistivities less than 80 Ohm-m. At depth in the profile, this response extends downward till the section limit between positions 30 and 95 m. In the interval 60 – 90 m it shallows and drapes down on a dome-like very low resistivity response. Lateral and vertical variations in the resistivity of this response are higher compared to that observed on Tr. 1. The resistivities are generally lower and vary over shorter distances and depth ranges. This response is again interpreted to represent the *in-situ* weathering topsoil at shallow levels and weathering remains of the original basement rock at the survey site at deeper levels. At either extremes of this profile, the response at depth consists of high resistivity values in excess of 230 Ohm-m. The northern segment of this high resistivity response occurs from a depth of about 2.5 m downwards. Its southerly limit is vertical while its upper limit dips towards the north. This dip possibly indicates of the presence of a trough-like depression similar to that observed in Tr. 1. The upper limit of the southern segment of this response occurs at a deeper level, from roughly 6 m downwards and is convex towards the surface (dome-like). This response is also interpreted as the un-weathered bedrock within the area. A third response occurs at depth from 60 m to 90 m along the profile. This pattern is a very low resistivity signature with values generally less than 82 Ohm-m. Its shallowest point is at 77 m where it extends from 5 m depth downwards. Its upper limit dips downwards on both sides of this peak forming a dome-like structure. This signature is further interpreted to represent either of the two possibilities suggested for the dome-like very low resistivity pattern on Tr. 1; in-situ clays filling weathering trenches or fracture subterranean fluid migration pathways.

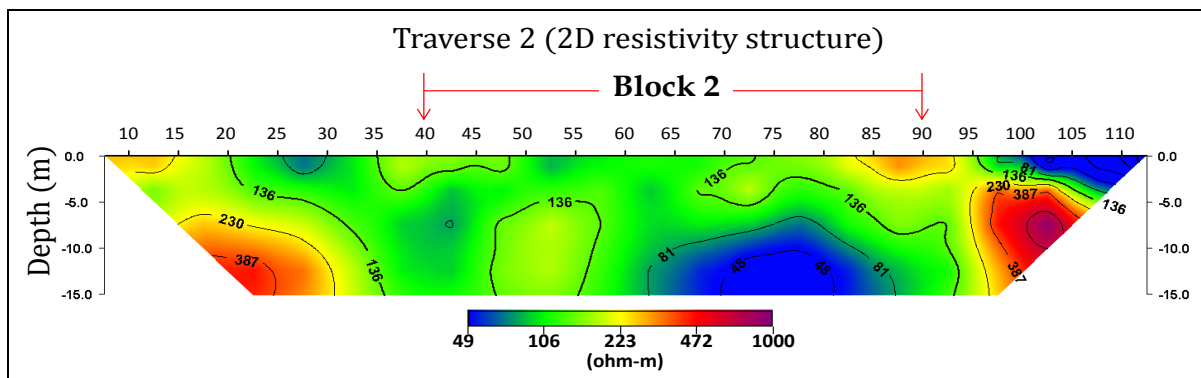


Fig. 4: Inverted 2D resistivity structure beneath Traverse 2. The traverse is dominated by moderate resistivity responses with the exceptions of the southern and northern limit where it presents with high resistivity responses and the dome shaped low resistivity response between positions 60 m and 87 along the traverse. Block 2 at depth straddles moderate and low resistivities at depth

Fig. 5 is the inverted 2D resistivity structure beneath Traverse 3 (Tr. 3) location. This traverse straddles east to west at a distance 1.2 m north of the front wall of the south block (Block 3) of the complex. In the shallow near-surface section of Tr.3, very low resistivity responses are dominant. This response exists as a laterally continuous pattern with its upper and lower limits undulating severely and paralleling one another for almost the entire profile. The response value is generally less than 82 Ohm-m. The upper limit of this response reaches to the surface from 25 – 30 m and from 55 m to the western limit of the profile. For most of the profile the upper limit is at a depth of 3 – 4 m but reaches to 6 m towards its eastern limit. The average thickness of this response is 7 m. This response is interpreted to represent deep-weathering water saturated *in-situ* clays in the area. This pattern is capped between position 30 m and 55 m along the profile by moderate resistivity responses (130 – 250 Ohm-m) which likely represent surficial topsoil at the site. In the eastern extreme of the profile, a wedge of high resistivity responses extends from the surface till a depth beyond 6 m. This response possibly represents dried-out clay-rich fractions of the topsoil at the site. At depths generally in excess of 10 m along the profile, moderate resistivity responses with resistivities in the range 130 – 250 Ohm-m dominate. The response is continuous and its upper surface undulates rapidly. Its undulation has likely informed the undulation of the

shallower low resistivity signature above it and could indicate rapid variations in weathering resistance of the original basement rock beneath the profile. This pattern is here interpreted to represent the weathered basement rock at the site. The bedrock along this profile has apparently experienced deeper weathering than along Tr. 1.

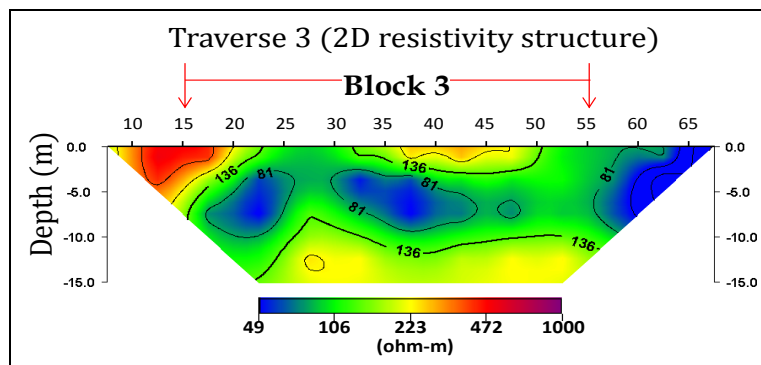


Fig. 5: Inverted 2D resistivity structure beneath Traverse 3. Undulations of the moderate and low resistivity patterns possibly indicate lateral variations in resistance to weathering of the original basement rock. Block 3 straddles low resistivity responses at depth.

Fig. 6 is the inverted 2D resistivity structure beneath Traverse 4 (Tr. 4) location. This traverse straddles east to west at a distance 1.2 m south of the rear wall of the south block (Block 3) of the complex. At depth, profile Tr. 4 is dominated by very low resistivity response (< 82 Ohm-m) patterns. The exceptions are two signatures of slightly higher resistivities just above 100 Ohm-m. The first is in the eastern extreme of the profile while the second vertically segments the very low resistivity response pattern in two. Both segments of the low resistivity response pattern have upper surfaces which are slightly depressed forming troughs. The western segment extends from an average depth of 4 m downwards while the eastern segment has an average upper limit 6 m beneath the ground surface. The eastern segment further extends to the surface between positions 15 m and 25 m. This low resistivity response is once again interpreted at deep-weathering clays at the site. In the near-surface interval, moderate resistivity responses exist nearly all-through the profile. This response pattern possesses resistivities in the range 130 – 250 Ohm-m and has an average thickness of 4 m. It drapes downwards above the low resistivity responses filling troughs on their upper limits. This response pattern is absent between positions 15 m and 25 m where it has been replaced by the upward extension of the low resistivity pattern. This pattern is interpreted as the surficial topsoil at the site.

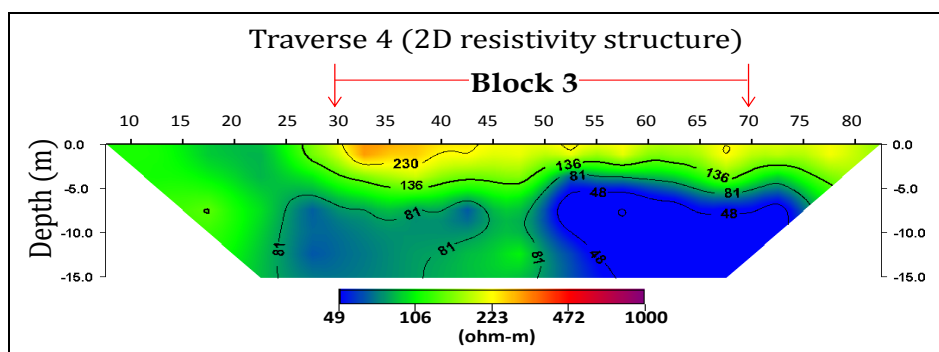


Fig. 6: Inverted 2D resistivity structure beneath Traverse 4. The low resistivity response pattern along the southern wall of Block 3 is much thicker and extends vertically from an average depth of 4 m till the limit of the section. Its upper limit also undulates similarly to that on Traverse 3.

VI. Discussion

The 2D inverted resistivity sections obtained for the surveys were arranged into a composite fence diagram to give a pseudo-3D representation of the subsurface electrical property distribution at the survey site (Fig. 7). It is likely that the high resistivity responses are continuous in the subsurface between Tr. 1 and the northern section of Tr. 2. In such a case, the survey site to the north and northeastern section would be underlain by the un-weathered basement rocks of the area. To the south and southwest, low resistivity deep-weathering water clays would generally predominate at depths in excess of 4 m. The exception could be in the southwest extreme of the area. The water saturated clays apparently emerge onto the site through a relatively narrow dome-shaped tunnel path in the west imaged along Tr. 2. This area adjoins the path of the seasonal stream

running N-S across the site. The water saturated clay response thereafter apparently fans out in a funnel-shaped fashion in the southeasterly direction. The morphology of the clay body changes rapidly. Along Tr. 2, the response extends from about 5 m from the surface to depths in excess of 15 m. Further south at Tr. 3, the response thins to about 7 m with its upper and lower limits undulating rapidly. Average depth range of its upper surface for most of the traverse is 3 – 4 m while its lower surface grades downwards into relatively more weathering resistant remains of the basement rocks. Further south at Tr. 4, the thickness of the clays increases considerably. Its upper limit averages a depth of 5 m from the surface and the response extends beyond the vertical limit of the section. This rapid variation in thickness could be related to variations in resistance to weathering of the original basement rocks of the area. Alternately, if the troughs have originated from fracture induced preferential weathering, the variations could be a reflection of the degree of fracturing that have generated these deep weathering sections and may also be the result of the amount of fluids such paths channel in the subsurface [8]. Whether the troughs are fracture induced or not has not been ascertained in this study. However, it is noteworthy, that the southern limits of the un-weathered basement at the site are vertical in the inverted resistivity sections, particularly on Tr. 1. This could be an indication of a fracture related origin. Also, the upper surface of the basement response on Tr. 1 in the proximity of this vertical basement scarp, presents as a concave upward trench. Similar near-scarp trenches have been reported in proximity to subsurface fracture induced basement scarps [8].

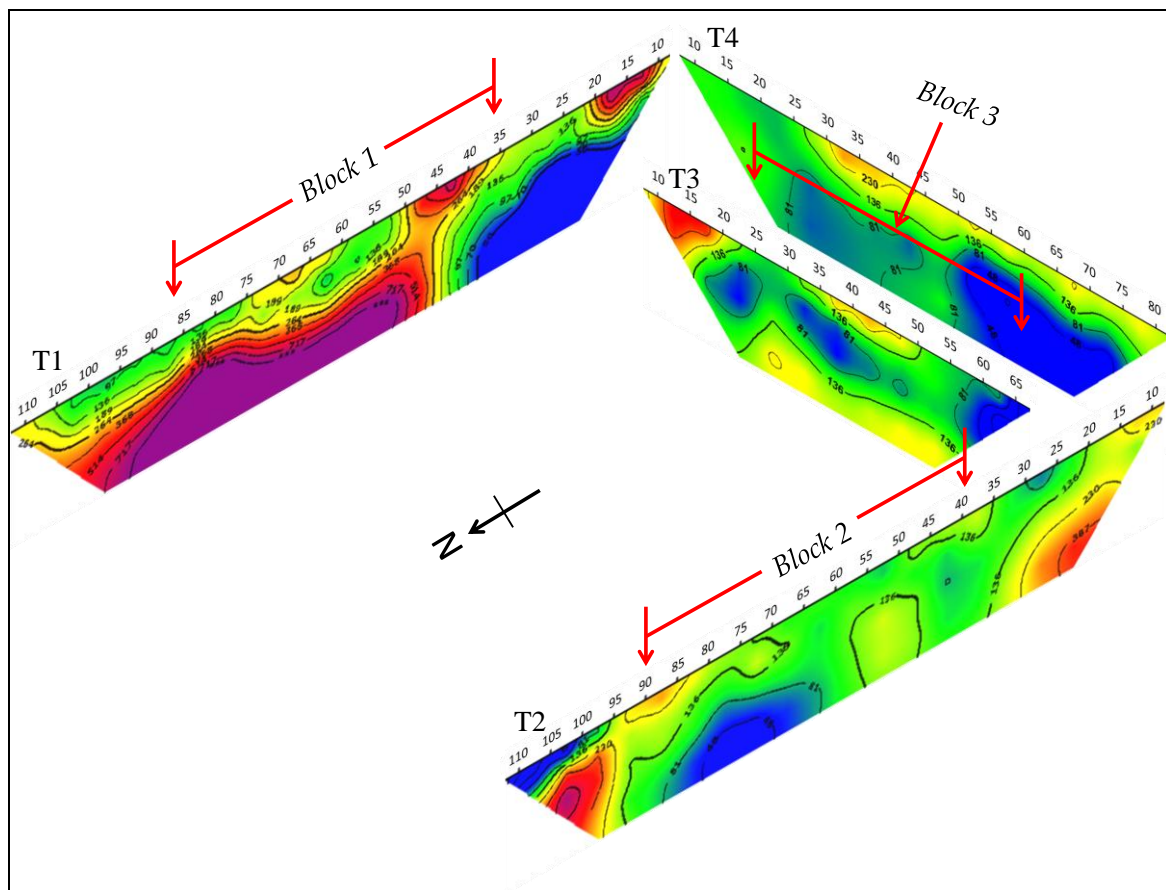


Fig. 7: Composite fence plot of all three traverses. In the northeastern sections, the site is dominated by high resistivity responses. The low resistivity response (blue) appears to emerge unto the site through a dome-shaped submerged section towards the northern end of Traverse 2 but quickly fans out covering most of the southern parts of the site. Refer to figure 1 for actual spatial separation between traverse.

Fig. 8 is the superposition of the field site layout upon the derived conceptual model of the subsurface at the survey location for an average depth beneath the surface of 5 m. For most of the site, the eastern administrative block of the complex sits upon basement rocks at depth, however, its southernmost end has been built across a vertical scarp-edge of the basement onto water saturated clays at depth. This has apparently informed a cantilever-style differential settlement of the building between the northern section which lies on thin topsoil above basement rocks and the southern section which lies at depth on water saturated clays. This is indicated by extensive hair-line cracks which have developed on the external walls and corridor pavements of the building. In the interior of this section which houses conveniences attached to the building, wide lateral and

vertical cracks have developed, and sections of the floor have begun to cave-in (Fig. 2f - g). This section is currently undergoing palliative repair measures. Block 3 apparently sits upon water saturated clays all through at depth, the clay section being thicker along the southern wall relative to the northern wall. Apparently, this building is also experiencing differential settlement. This explains the hair-line cracks which have developed on both its internal and external wall, particularly in doorways and on window frames. Block 2 possibly spans water saturated clays and deep weathering tills. The water saturated clays along this profile at depth is relatively narrower and deeply buried. This perhaps explains why this building is yet to develop any sign of foundation related failure. At least no visible cracks have been noticed on this block. Much cannot however be said of the future. As utilization progresses, it will be necessary to closely monitor this building for possible signs of distress.

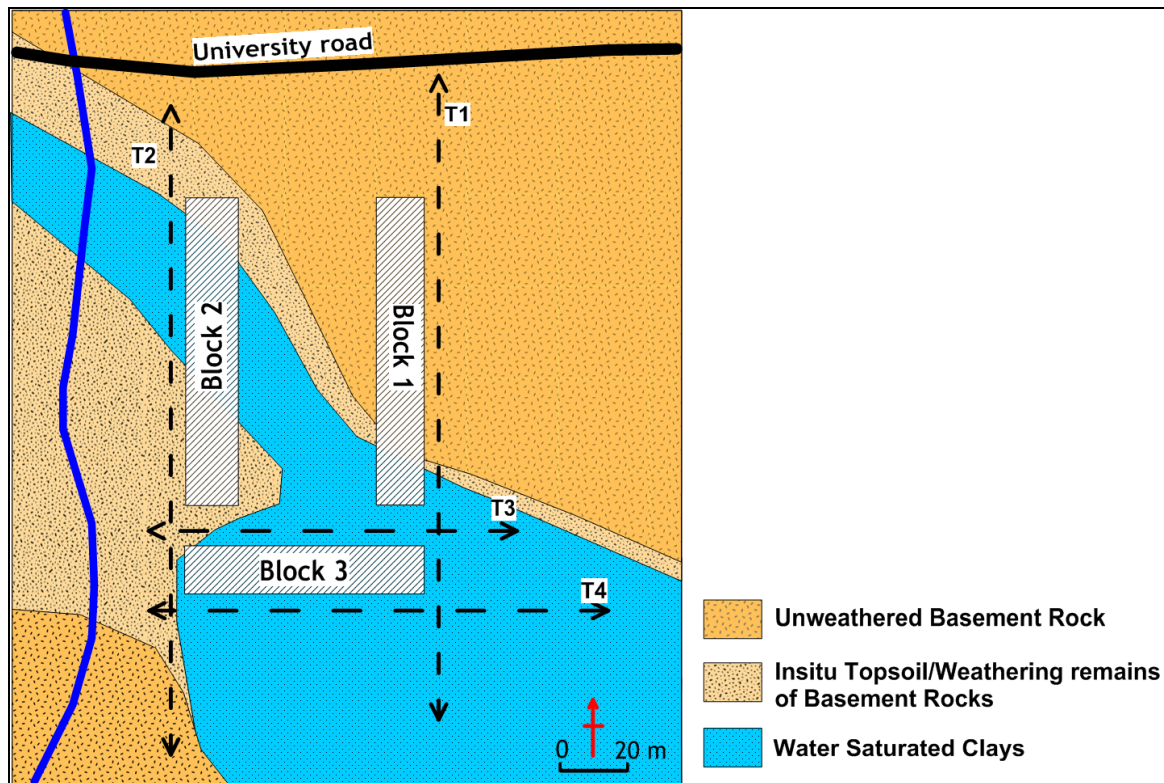


Fig. 8: Conceptual subsurface model of the study area at an approximate depth of 6 m beneath the ground surface. Block 1 has been built over the edge of the un-weathered basement onto inferred water saturated clays leading to differential settling of the conveniences section of building and the resulting damage. Block 3 sits at depth entirely on water saturated clays with differential settling resulting from difference in thickness of the clays along its north facing and south facing walls.

VII. Conclusion

Electrical resistivity imaging has been used to investigate subsurface conditions around a set of administrative blocks which have developed extensive wall cracks on the Adekunle Ajasin University Campus, southwestern Nigeria. Block 1, the more damaged building has been built across a scarp in the underlying basement rock onto thick water saturated clays. This situation has resulted in differential settling of the building and the consequent development of wall cracks and floor cave-ins. The southerly block rest entirely upon water saturated clays and although apparently settling differentially, the development of cracks are not as severe as on Block 1. The water saturated clays span the entire southwestern portion of the site and could be fracture related. Water supply to the system likely comes through a submerged dome-shaped section adjacent to the seasonal stream course. Although the results of this study have not been calibrated to core or geotechnical pitting data, a good appreciation of the subsurface geologic conditions at the site and insight into the possible causes of the emergence of structural failure indices on the administrative buildings have been obtained. The study underscores the value of geophysical investigations to construction site evaluation even in the absence of geotechnical data.

Acknowledgements

I am grateful to Abimbola Raji and Tola Ayodele both formerly of the Department of Earth Sciences, Adekunle Ajasin University, Akungba-Akoko, Nigeria, for assistance rendered in the collection of field resistivity data.

References

- [1] P. M. Soupios, P. Georgakopoulos, N. Papadopoulos, V. Saltas, A. Andreadakis, F. Vallianatos, A. Sarris, A., and J. P. Makris, Use of engineering geophysics to investigate a site for a building foundation, *Journal of Geophysics and Engineering*, 4(1), 2007, 94–103.
- [2] P. Cosenza, E. Marmet, F. Rejiba, Y. J. Cui, A. Tabbagh, and Y. Charlery, 2006, Correlations between geotechnical and electrical data: A case study at Garchy in France, *Journal of Applied Geophysics*, 60(3), 2006, 165–178
- [3] N. Anderson, N. Croxton, R. Hoover, and P. Sirles, *Geophysical Methods Commonly Employed for Geotechnical Site Characterization*, Transportation Research Circular, Transportation Research Board of the National Academies, E-C130, 2008, P. 43.
- [4] M. H. Loke, *Electrical imaging surveys for environmental and engineering studies: a practical guide to 2-D and 3-D surveys*, 2000, <http://www.heritagegeophysics.com/images/lokenote.pdf>.
- [5] E. Rizzo, A. Colella, V. Lapenna, and S. Piscitelli, High-resolution images of the fault-controlled High Agri-Valley basin (Southern Italy) with deep and shallow electrical resistivity tomographies. *Physical Chemistry of the Earth*, 29 (4), 2004, 321–327.
- [6] F. Nguyen, S. Garambois, D. Jongmans, E. Pirard, and M. H. Loke, Image processing of 2D resistivity data for imaging faults. *Journal of Applied Geophysics*, 57(4), 2005, 260–277.
- [7] K. M. Bufford, E. A. Atekwana, and M. G. Abdelsalam, Geometry and faults tectonic activity of the Okavango Rift Zone, Botswana: evidence from magnetotelluric and electrical resistivity tomography imaging. *Journal of African Earth Sciences*, 65, 2012, 61–71.
- [8] M. B. Aminu, T. M. Akande, and A. O. Ishola, 2D Geoelectric Imaging of the Uneme-Nekhwa Fracture Zone. *Hindawi Publishing Corporation, International Journal of Geophysics*, 2014, Article ID 842812, 8 pages <http://dx.doi.org/10.1155/2014/842812>
- [9] R. E. Chávez, G. Cifuentes-Nava, A. Tejero, J. E. Hernández-Quintero, and D. Vargas, Special 3D electric resistivity tomography (ERT) array applied to detect buried fractures on urban areas: San Antonio Tecómitl, Milpa Alta, México. *Geofísica Internacional* 53(4), 2014, 425-434
- [10] B. Robineau, J. L. Join, A. Beauvais, J-C. Parisot, and C. Savin, 2007, Geoelectrical imaging of a thick regolith developed on ultramafic rocks: groundwater influence. *Australian Journal of Earth Sciences*, 54(5), 2007, 773-781.
- [11] M. B. Aminu, Electrical Resistivity Imaging of a Thin Clayey Aquitard Developed on Basement Rocks in Parts of Adekunle Ajasin University Campus, Akungba-Akoko, South-western Nigeria. *Environmental Research, Engineering and Management*, 71(1), 2015, 47 – 55.
- [12] G. El-Qady, M. Hafez, M. A. Abdalla, and K. Ushijima, Imaging subsurface cavities using geoelectric tomography and ground penetrating radar, *Journal of Cave and Karst Studies*, 67(3), 2005, 174–181.
- [13] J. P. Lines, S. Bernardes, J. He, S. Zhang, S. T. Bacchus, M. Madden, and T. Jordan, 2012, Preferential Groundwater Flow Pathways and Hydroperiod Alterations Indicated by Geo-rectified Lineaments and Sinkholes at Proposed Karst Nuclear Power Plant and Mine Sites. *Journal of Sustainable Development*, 5(12), 2012, 78-116.
- [14] R. R. Yassin, R. F. Muhammad, S. H. Taib, and O. Al-Kouri, 2014, Application of ERT and Aerial Photographs Techniques to Identify the Consequences of Sinkholes Hazards in Constructing Housing Complexes Sites over Karstic Carbonate Bedrock in Perak, Peninsular Malaysia. *Journal of Geography and Geology*, 6(3), 2014, 55-89.
- [15] J. T. Zume, A. Tarhule, and S. Cristenson, Subsurface imaging of an abandoned solid waste landfill site in Norman, Oklahoma, *Ground Water Monitoring and Remediation*, 25(2), 2006, 62-69.
- [16] V. Frid, G. Liskevich, D. Doudkinski, and N. Korostishevsky, Evaluation of landfill disposal boundary by means of electrical resistivity imaging. *Environmental Geology*, 53(7), 2007, 1503-1508.
- [17] M. A. Rahaman, Review of the Basement Geology of South-Western Nigeria, in: C. A. Kogbe (Ed), *Geology of Nigeria*, (Nigeria: Rock View Limited 1989) 39-56.
- [18] M. J. Yi, and J. H. Kim, Enhancing the resolving power of the least squares inversion with Active Constraint Balancing: SEG Expanded Abstracts, 68 Annual Meeting, New Orleans, 1998, 485-488.